

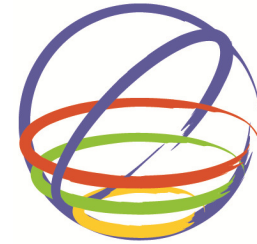
# Development of Fragility Functions for Low Strength Masonry Buildings in Nepal using Applied Element Method

**R. Guragain & A.M. Dixit**

*National Society for Earthquake Technology-Nepal (NSET), Nepal*

**K. Meguro**

*Institute of Industrial Science, The University of Tokyo, Japan*



**15 WCEE**  
LISBOA 2012

## SUMMARY

Earthquake risk assessment and preparation of earthquake risk scenario is a strong awareness raising and planning tool for implementing earthquake risk management activities. Use of appropriate fragility functions is one of the most critical parameters for the accuracy of earthquake risk assessment. This study computed fragility functions for non-engineered low earthquake resistant masonry buildings in Nepal through non-linear analysis using Applied Element Method (AEM). Key parameters required for analysis were obtained through field test in actual field condition. Results obtained from AEM were compared with shaking table experiment and a good agreement was found. Buildings with different configuration, material strength, the number of stories and mortar type were subjected to numerical simulation and probability of damage exceeding a certain level of damage state is calculated for peak ground acceleration (PGA) starting from 0.05g to 1.0g. Fragility functions for low earthquake resistant masonry buildings for different state of damage are plotted based on numerical simulation results.

*Keywords: masonry buildings, fragility functions, Applied Element Method, time history analysis*

## 1. INTRODUCTION

Earthquake risk evaluation is the first step for realistic and effective planning and implementation of earthquake risk reduction as well as preparedness initiatives as it helps understanding the underlying problems and its magnitude. Either simple earthquake loss estimation based on secondary information on seismic hazards and vulnerabilities or detail quantitative analysis of individual buildings and infrastructures, the risk assessment has been a very strong awareness raising and planning tool for implementing earthquake risk management activities in developing countries (Guragain et al., 2008).

Use of appropriate fragility functions for specific type of buildings is one of the main parameters for earthquake risk evaluation. Coburn, A. and Spence, R. (2002) give the breakdown of the fatalities due to earthquakes in the period of 1900-1990 in the world and about 75% of the fatalities attributed to earthquakes are caused by the collapse of buildings and the greatest proportion is from the collapse of masonry buildings. This trend has been continued in recent earthquakes in developing countries as well. So, the accuracy of earthquake loss estimation depends more on accuracy of fragility functions of masonry buildings.

Different fragility functions/curves for masonry buildings in developing countries are suggested by various methods and authors like ATC-13(1985), Arya et al. (1994), RADIUS(2000) and GESI(2001) and are in use in Nepal for earthquake risk assessment at cities (Guragain et al., 2008). All these methods give a single fragility curve defining potential damage ratio at a certain level of earthquake shaking for one type of buildings and do not differentiate different state of damage at the given level of shaking. New earthquake risk assessment tools like HAZUS (HAZUS, 2003) gives a set of fragility functions like slight, moderate, extensive and complete damage for masonry buildings. However, these fragility functions are for buildings in United States and similar fragility functions for masonry

buildings in Nepal are not available.

This study focuses on development of a set of fragility functions for masonry buildings in Nepal so that earthquake risk assessment can be done for different level of damage. Essential parameters required for numerical simulation are collected through field test and fragility functions are developed through numerical simulation using Extreme Loading for Structures (ELS) computer software developed in Applied Element Method(AEM) platform.

## 2. FIELD TEST OF EXISTING MASONRY BUILDINGS

Reliable information on shear resistance is needed when performing retrofits and seismic upgrades of masonry buildings. The shear strength of a masonry wall is difficult to measure without resorting to large-scale testing. Destructive test for evaluating shear strength of the whole masonry wall of existing buildings is not possible in a large scale. As an alternative less destructive in-place tests of single masonry units provide a comparative figure that can be correlated to full-scale wall behavior (ASTM C1531-09). This less destructive alternative is more economical than large-scale testing and is desirable when a building's existing integrity must be maintained. The in-place shear test is also known as the push test. It provides a direct measurement of the shear resistance of mortar joints in masonry. The test is suitable for masonry that has relatively strong units and weak mortar so that shear cracks form in the typical stair step pattern along mortar joints and the units remain un-cracked. In this type of construction, the shear strength of the mortar joints limits the shear strength of the masonry wall.

Hydraulic hand pump by Hi Force company model number HP 110 which has the capacity of 700 bar force was used as the equipment for the test. ASTM C1531-09 was used for conducting the field tests in Nepal and Bangladesh. Table 2.1.1 gives the steps followed for conducting the tests. Table 2.1.2 gives the test results for cement mortar and mud mortar masonry.

**Table 2.1.1:** Steps for conducting direct shear test at field

Steps	Actions
Step 1	Selection brick for direct shear test: A wall panel with minimum of 8 full bricks in horizontal and 11 layers of bricks in vertical is selected to avoid any other patterns of failure. Two bricks are marked at centre horizontally and at the base of the selected wall panel.
Step 2	Remove plaster from two selected bricks.
Step 3	Remove one of the brick and a vertical joint using drill machine.
Step 4	Keep Hi-Force Jack in the cavity with steel bearing plates in proper position.
Step 5	Apply pressure by hydraulic pump manually and observe pressure value along with failure mode.

**Table 2.1.2:** Direct shear test result

Parameters	Cement Mortar	Mud Mortar
Number of tests	35	17
Median value of corrected shear strength (N/mm <sup>2</sup> )	0.723	0.106
Standard Deviation	0.342	0.106
20th Percentile of corrected shear strength (N/mm <sup>2</sup> )	0.455	0.0716
80th Percentile of corrected shear strength (N/mm <sup>2</sup> )	0.988	0.1478

## 3. NON LINEAR SIMULATION

One way of developing fragility functions is through damage assessment after a real earthquake disaster and it is required to wait for a large earthquake to occur. The other way is through numerical simulations. Authors like M. Rota et al. (2010) and J. Park et al. (2009) have developed fragility functions for different types of buildings through macro modelling. In case of masonry, as the main

energy dissipation is through cracking as well as frictional sliding, micro modelling after cracking with bricks and mortar is required. In the domain of numerical simulation of masonry buildings, the AEM is more suitable than other approaches because of mainly three reasons. Firstly, the AEM is capable to follow complete structural response from initial stage of loading until total collapse behaviour with reasonable accuracy so that inelastic responses after the cracks occur can be captured (Meguro K. and Tagel-Din H, 2001). Secondly, brick masonry which is composite of brick units and mortar and has discrete nature can easily be model in the AEM by a set of square elements connected at their contact edges either by 'Element springs' or 'Joint springs' according to their positions (Guragain, R. et al. 2006). Thirdly, the progressive failure of masonry i.e. cracks initiation, propagation and their distribution is simulated better by AEM (Guragain, R. et al. 2006).

AEM has shown good results for analysis for different types of loading. AEM has been used to simulate the behavior of masonry by Pandey et al. (2004) and Mayorca et al. (2004) for monotonic load case, Guragain et al. (2006) for cyclic loading 2-D and Worakanchana et al. (2010) for cyclic loading 3-D. Applied Science International, LLC (ASI), has developed a structural analysis tool called Extreme Loading for Structures (ELS) in AEM. The ELS software has been used for this study for Time History analysis of masonry buildings.

### 3.1. Experimental Verification

The ELS software was first used for an experimental model to verify the analysis result with the experimental data. The shaking table test conducted by Sathiparan, N. (2008) in the Meguro Laboratory at the University of Tokyo was used for verification of numerical result obtained from ELS. Model A-4-NR-X which was for non-retrofitted without plaster Adobe model was chosen for numerical simulation.

#### 3.1.1. Model Parameters

The specimen was made of 18 rows of 44 bricks in each layer except openings. Typical parameters of the building model and materials used are given in Table 3.1.1. Figures 3.1.1 and 3.1.2 give the photograph of experimental model and the numerical model prepared for ELS, respectively. The overall dimension of model without roof was 933mm x 933mm x 720 mm and the wall thickness was 50mm. The sizes of door and window in opposite walls were 243mmx485mm and 325mmx245mm, respectively. In case of numerical model, the roof is simulated just by a layer of wooden beam as top layer which has assigned to same weight of the roof in experiment.



**Figure 3.1.1:** Experimental model  
(Sathiparan, N., 2008)

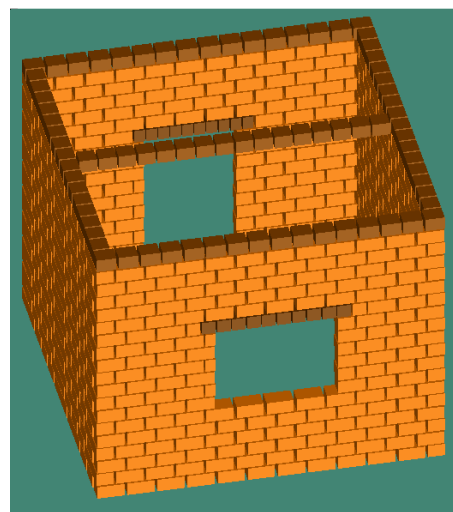


**Figure 3.1.2:** Numerical model

### 3.1.2. Input Motions

Sinusoidal motions of frequencies ranging from 2Hz to 35Hz and amplitudes ranging from 0.05g to 0.8g were applied to obtain the dynamic response of the structures in the experiment. Figure 3.1.3 shows the typical shape of the applied sinusoidal wave.

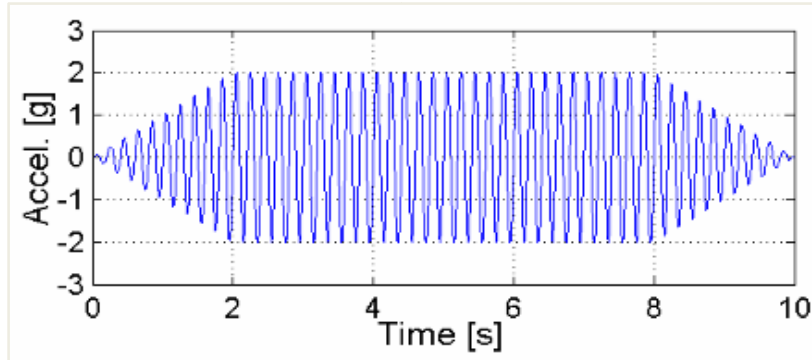


**Figure 3.1.3:** Typical shape of the applied sinusoidal wave

The numbers given in the Table 3.1.1 show the loading sequence followed for tests. General trend of loading was from high frequency to low frequency and from lower amplitude to higher amplitude. There was no significant damage to run 22, thus, the numerical simulation was performed only from run 22 to run 45. During experiment, there was some gap between consequent run so that the model was in a static condition before another run of input motion. However, in case of numerical simulation the input motion was continuously provided one after another.

**Table 3.1.1:** Loading sequence of input motions

Amplitude	Frequency							
	2Hz	5Hz	10Hz	15Hz	20Hz	25Hz	30Hz	35Hz
0.8g			43	40	37	34	31	28
0.6g		45	42	39	36	33	30	27
0.4g		44	41	38	35	32	29	26
0.2g		25	24	23	22	21	20	19
0.1g	18	17	16	15	14	13	12	11
0.05g	10	09	08	07	06	05	04	03
sweep	01,02							

### 3.1.3. Result Comparison

The result of the experiment in terms of cracks patterns and extent of damage which are documented by Sathiparan, N.(2008) are compared with simulation result. The comparison of the results is done after run 28, 37 and 45.

Figure 3.1.4 shows the crack patterns mapped after run 28 of the experiment. A large crack was observed in one top corner of the door. We could also observe some cracks at the bottom layer of the side of the door, cracks in all four corners of the window and some horizontal cracks near to the top layer to other sides than the window and the door. Figure 3.1.5 shows the crack patterns after run 28 from numerical simulation. Cracks were observed in both sides of the top corners of the door with one crack longer and another shorter similar to the experimental cracks. Similarly, cracks in all four corners of the window were observed and are found similar to the experimental result. The cracks at top corners of the windows reach to the top layer of the bricks.

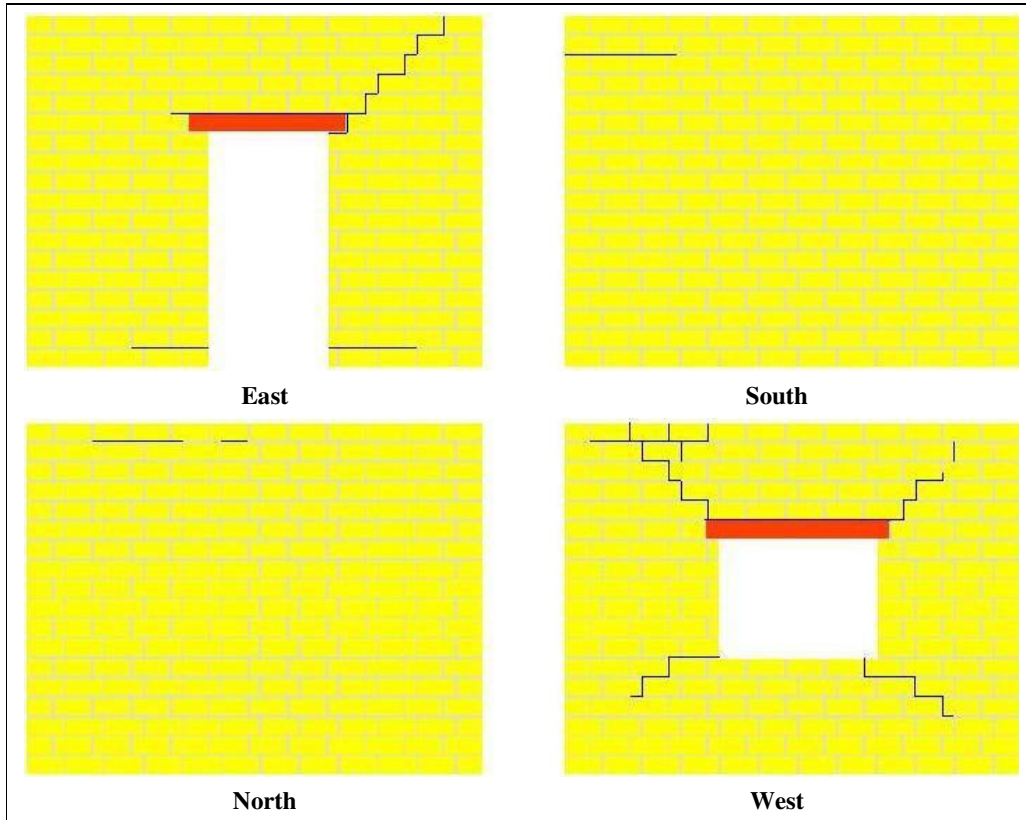


**Figure 3.1.4:** Crack pattern after run 28 (35Hz-0.8g) from experiment (Sathiparan, N., 2008)

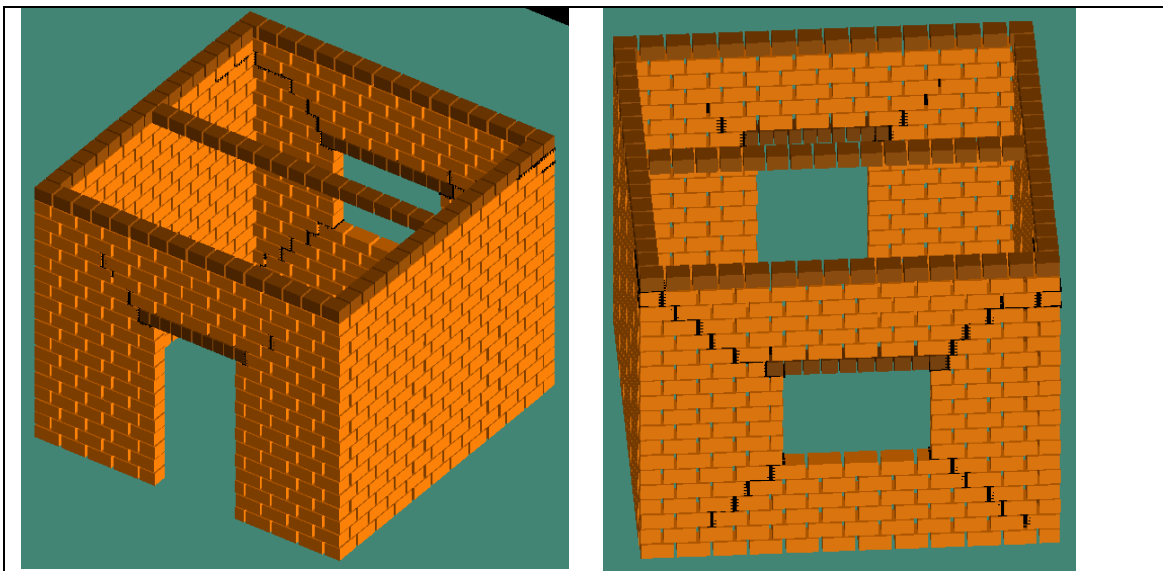


**Figure 3.1.5:** Crack patterns after run 28 (35Hz-0.8g) from numerical simulation

Figures 3.1.6 and 3.1.7 show crack patterns after run 37 from experiment and numerical simulation, respectively. In both the cases, there are more cracks above the openings, more horizontal cracks in side walls and the horizontal cracks at the top layer of the side walls almost passes through one side to the other.

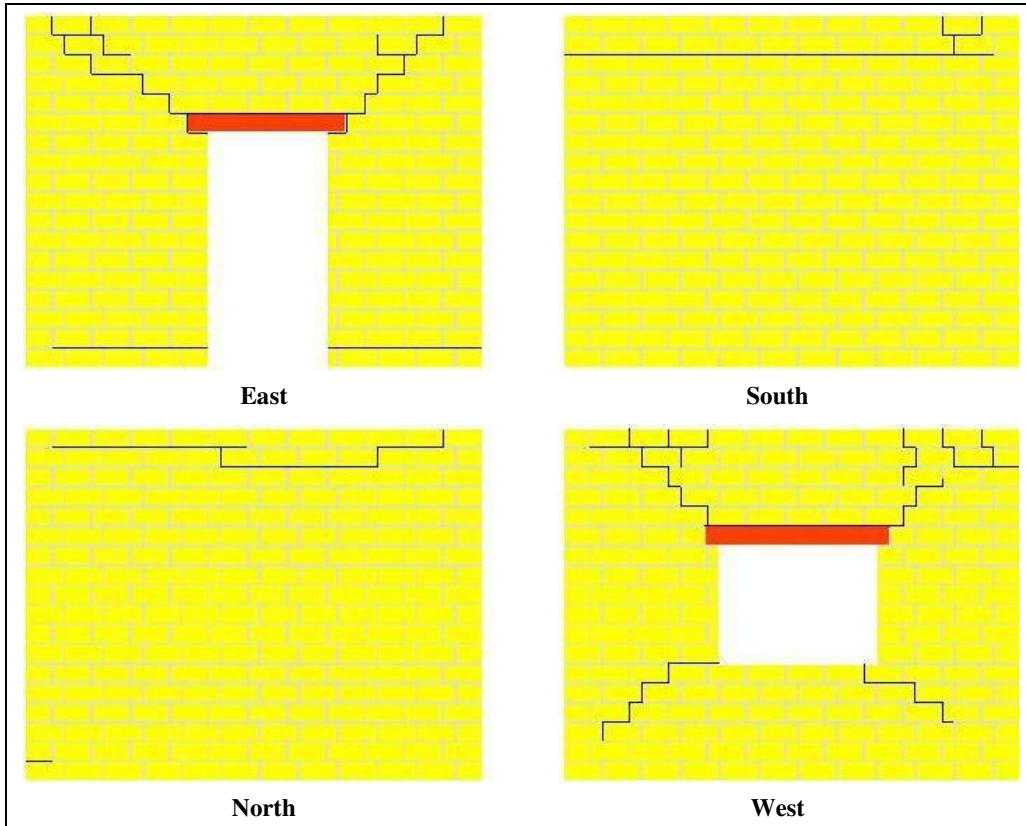


**Figure 3.1.6:** Crack patterns after run 37 (20Hz-0.8g) from experiment (Sathiparan, N., 2008)

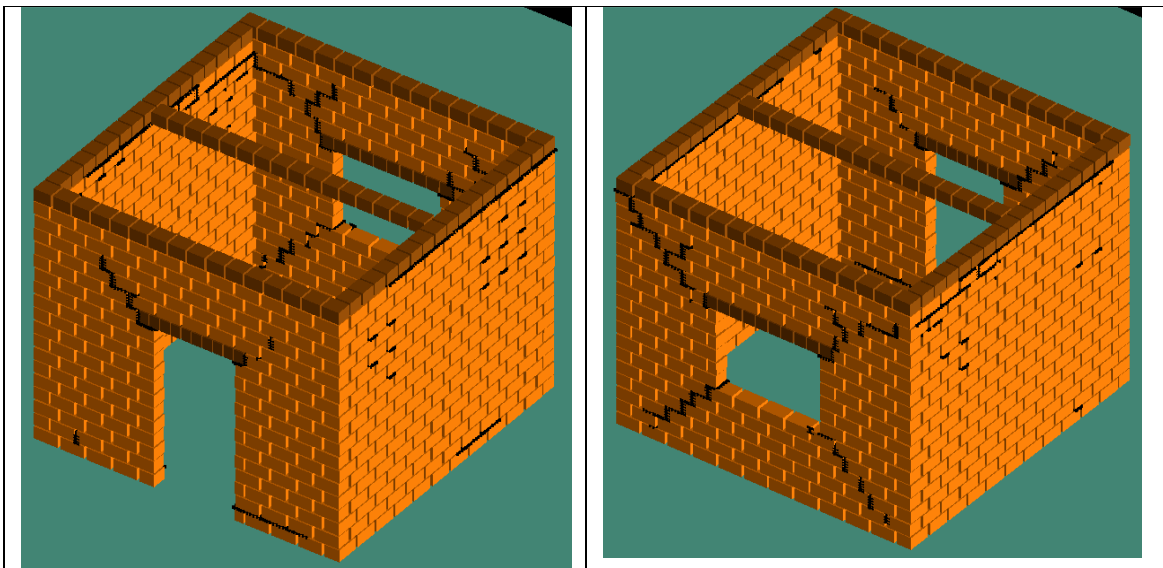


**Figure 3.1.7:** Crack patterns after run 37 (20Hz-0.8g) from numerical simulation

Figures 3.1.8 and 3.1.9 show the photographs of the experiment model after the final run 45 (5HZ-0.6g) and Figures 3.1.10 and 3.1.11 show the numerical simulation results after the same run. In both the experimental and numerical cases, the masonry wall above the door and window is collapsed.

Similarly, some portion of side walls has also fallen in both cases. In the experiment as well as numerical simulation, the initial cracks widened in further shaking ultimately leading to collapse. This behaviour is typical of non-retrofitted masonry buildings which has very limited ductility. So, the energy dissipation capacity is limited as there are few but large cracks.

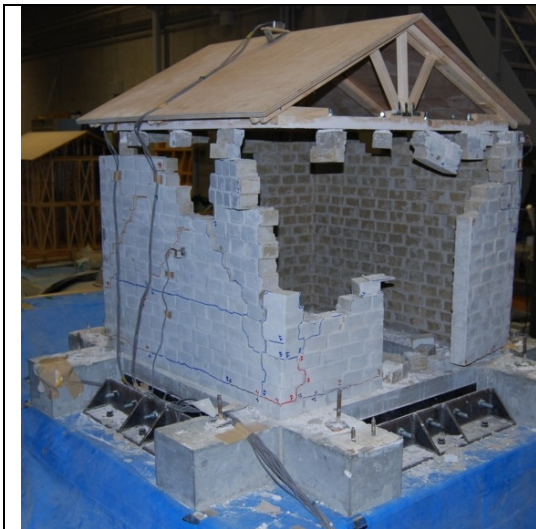


**Figure 3.1.10:** Door side photo after run 45 (5HZ-0.6g) of experiment (Sathiparan, N. 2008)

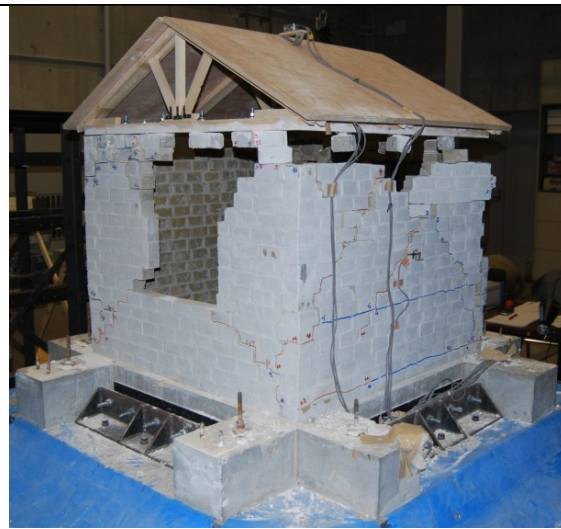


**Figure 3.1.11:** Window side photo after run 45 (5HZ-0.6g) of experiment (Sathiparan, N. 2008)

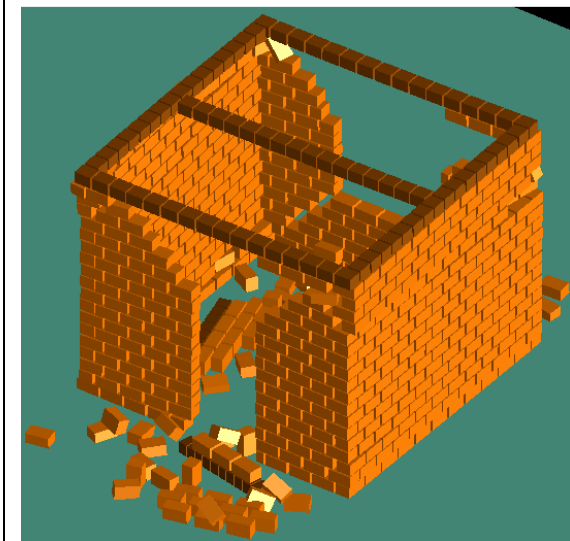


**Figure 3.1.12:** Numerical simulation result after run 45 (5HZ-0.6g) graphics from door side

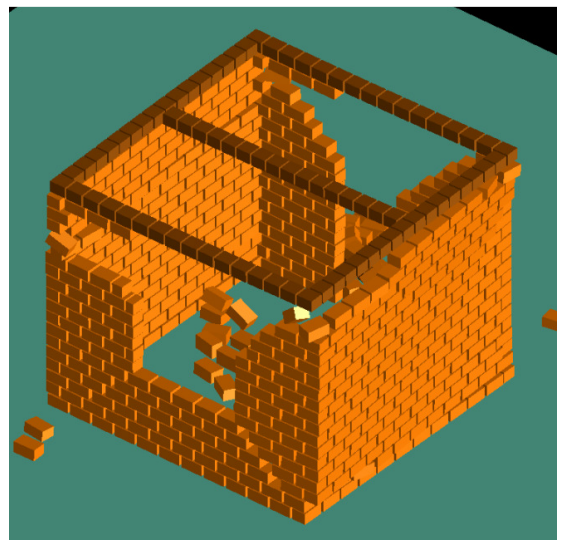


**Figure 3.1.13:** Numerical simulation result after run 45 (5HZ-0.6g) graphics from window side

The comparison of experimental and numerical results at different stages of loading shows a good agreement in the cracks initiation, propagation and also the collapse of masonry structure even though the numerical model was slightly simplified, especially the roof.

After this experimental verification, the ELS, market available AEM software, is used for numerical simulation of the masonry buildings in Nepal and Bangladesh for the development of fragility functions.

### 3.2. Time History Analysis and Formulation of Fragility Functions

Different types of masonry buildings with different wall thickness, the number of storey, flexible/rigid roofs are analysed under different acceleration input conditions. Each building is subjected to different level of input motions starting from 0.05g to 1.0g of peak ground acceleration (PGA) until the building completely damaged. About 60% of the models are analysed with median mortar strength given in Section 2 of this paper and about 20% with low mortar strength (20th percentile mortar strength) and about 20% with high strength (80th percentile mortar strength)

Level of damages: slight, moderate, extensive or complete are defined after each analysis based on cracks distribution and level of damage as per HAZUS (2003). 17 different cases with different building models, different mortar strength and different earthquakes are analysed to plot the fragility functions. Table 3.2.1 presents the result of analysis for different levels of time history accelerations. Slight, moderate, extensive and complete damage states are assigned observing the damage according to the HAZUS damage descriptions.

**Table 3.2.1:** Damage states of different models for different values of time history

Case	Building Information	Peak Ground Acceleration (g)									
		0.05	0.1	0.2	0.3	0.4	0.6	0.8	0.9	1	
1	D01_TH: 1 Story, Average Cement Mortar	N	S	S	M	E	C	C	C	C	
2	D01_TH: 1 Story, Average Cement Mortar	N	S	S	M	E	C	C	C	C	
3	D01_TH: 1 Story, Average Cement Mortar	S	S	M	E	E	C	C	C	C	
4	D01_TH: 1 Story, Average Cement Mortar	S	S	M	E	E	C	C	C	C	
5	D05_TH: 1 Story, Average Cement Mortar	N	S	S	M	M	E	E	C	C	
6	D05_TH: 1 Story, Average Cement Mortar	N	S	S	M	M	E	E	C	C	
7	C10_TH: 1 Story, Weak Cement Mortar	S	M	E	E	C	C	C	C	C	
8	C10_TH: 1 Story, Weak Cement Mortar	S	M	E	E	C	C	C	C	C	
9	C10_TH: 1 Story, Average Cement Mortar	S	M	E	C	C	C	C	C	C	
10	C10_TH: 1 Story, Average Cement Mortar	S	M	E	C	C	C	C	C	C	
11	S06_TH: 1 Story, Average Cement Mortar	S	S	M	M	E	C	C	C	C	
12	S06_TH: 1 Story, Average Cement Mortar	N	S	S	M	M	E	C	C	C	
13	D05_TH: 1 Story, Cement Strong Mortar	N	S	S	M	M	E	E	E	C	
14	D05_TH: 1 Story, Cement Strong Mortar	N	S	S	M	M	E	E	E	C	
15	S06_TH: 1 Story, Cement Strong Mortar	N	N	N	S	S	M	M	M	E	
16	NP01_M: 2 Story, Mud Weak Mortar, Rigid Slab	M	E	E	C	C	C	C	C	C	
17	NP02_M: 2 Story, Mud Weak Mortar, Flexible roof	E	C	C	C	C	C	C	C	C	

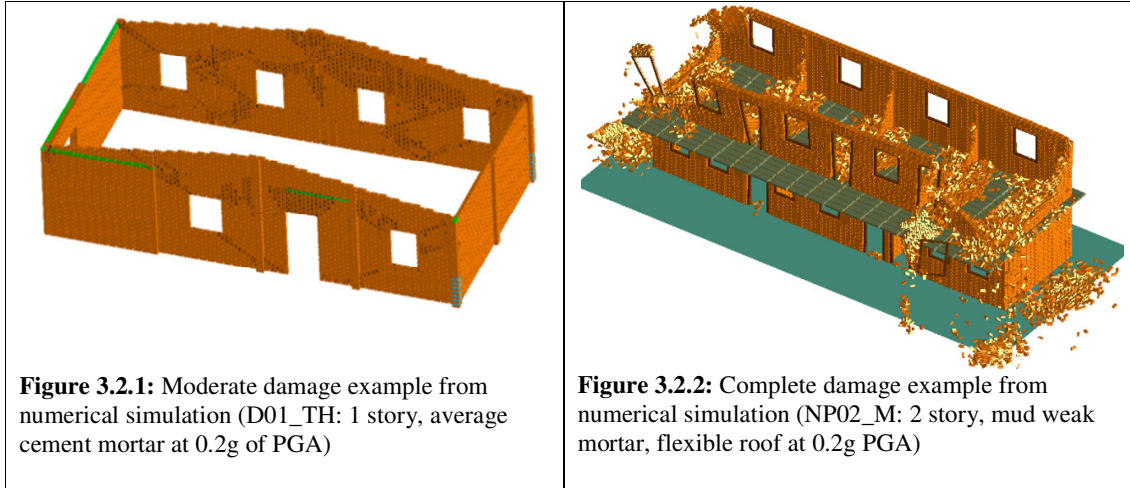
N: negligible damage; S: slight damage, M: moderate damage, E: extensive damage, C: complete damage

Cumulative probabilities of different level of damage states are calculated considering these 17 cases and are given in Table 3.2.2.

**Table 3.2.2:** Probabilities of particular or higher damage states at different input accelerations

Damage States	Peak Ground Accelerations (g)									
	0.05	0.1	0.2	0.3	0.4	0.6	0.8	0.9	1	
Slight	0.29	0.94	0.94	1.00	1.00	1.00	1.00	1.00	1.00	
Moderate	0.06	0.35	0.53	0.94	0.94	1.00	1.00	1.00	1.00	
Extensive	0.06	0.12	0.29	0.47	0.65	0.94	0.94	0.94	1.00	
Complete	0.00	0.06	0.06	0.24	0.35	0.65	0.71	0.82	0.94	

Figures 3.2.1 and 3.2.2 show the moderate damage example and complete damage example, respectively at the same level of ground acceleration of 0.2g. One storey building with average cement mortar strength has suffered moderate damage while two-storey building with flexible roof and low strength mud mortar has suffered complete damage with significant portion of the second floor collapsed.



Cumulative probabilities of different levels of damage states from Table 3.2.2 are plotted in relation to PGA and exceeding probability of a certain state of damage and fragility curves are fitted with lognormal distribution. Figure 3.2.3 gives the final outcome of this study in the form of fragility functions for low rise unreinforced masonry buildings in Nepal.

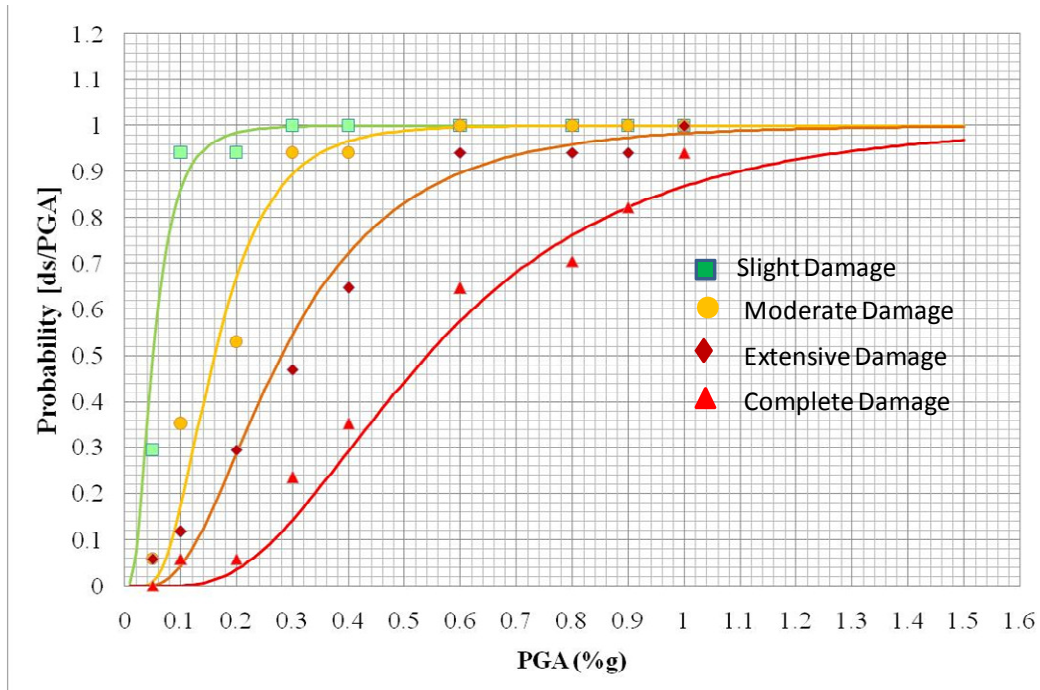


**Figure 3.2.3:** Numerically developed fragility functions for low-rise unreinforced masonry buildings in Nepal

#### 4. CONCLUSIONS AND RECOMMENDATIONS

Computation of fragility functions for non-engineered unreinforced low seismic capacity masonry buildings in Nepal through time history analysis using ELS tool developed based on the AEM was done. Key parameters required for non-linear analysis like shear strength of existing masonry buildings were obtained through direct shear test in actual field condition. The results obtained by the AEM were compared with shaking table test results and a good agreement between experimental and numerical results was found. Different buildings with different configuration, material strength, the number of stories and mortar type, total of 17 cases, were subjected to numerical simulation and probabilities of damage exceeding a certain level of damage state are calculated at 9 different levels of PGA starting from 0.05g to 1.0g. The level of damage was highly influenced by the number of stories, mortar strength and the roof and floor type and configuration. One storey building with strong cement mortar suffered only moderate damage at 0.4g but two-story building with weak mud mortar and flexible roof suffered complete damage at 0.1g. It is found that there is a large difference of damage with different parameters of the building. Preparation of different set of fragility functions for different types of masonry buildings, for example one set of functions for single storey mud mortar buildings with flexible floors, is recommended.

#### ACKNOWLEDGEMENT

The authors acknowledge the opportunity provided by National Society for Earthquake Technology-Nepal (NSET) for allowing to use the field test database conducted by authors for different projects and programs. We are also thankful to the Government of Japan, JSPS/ROKPAKU program for providing fellowship to the first author for conducting this research. We would like to thank to Applied Science International, LLC (ASI) for providing the academic licence of ELS software which was used for numerical simulation of masonry buildings.

#### REFERENCES

- ATC-13(1985), Earthquake Damage Evaluation Data for California, *Applied Technology Council*, 1985.
- A. S. Arya and TEAC Consult(1994), Appendix C: Seismic Vulnerability Analysis, *The Development of Alternative Buildings Material and Technology for Nepal*, 1994.
- RADIUS(2000) Risk Assessment Tools for Diagnosis of Urban Areas against Seismic Disasters. Geneva, Switzerland: IDNDR Secretariat, United Nations.
- GESI(2001): Global Earthquake Safety Initiative Pilot Project, Final report, GHI and UNCRD.
- Meguro K. and Tagel-Din H. (2001). Applied Element Simulation of RC Structures under Cyclic Loading. *Journal of Structural Engg.*;127(11):1295-1305
- Coburn, A. and Spence, R. (2002). *Earthquake protection*. West Sussex: John Wiley & Sons Ltd.
- HAZUS (2003), Multi-hazard Loss Estimation Methodology: Earthquake Model, Department of Homeland Security, Emergency Preparedness and Response Directorate FEMA, Washington D.C
- Mayorca, P. and Meguro, K., (2004). Proposal of an Efficient Technique for Retrofitting Unreinforced Masonry Dwellings. *Proceedings on 13<sup>th</sup> World Conference on Earthquake Engineering*, Vancouver, Canada.
- Pandey, BH. and Meguro, K. (2004). Simulation of Brick Masonry Wall Behavior under Inplane Lateral Loading Using Applied Element Method. *Proceedings on 13<sup>th</sup> WCEE*, Vancouver, Canada. 2004.
- Ramesh GURAGAIN, Kawin WORAKANCHANA, Paola MAYORCA and Kimiro MEGURO (2006); Simulation of Brick Masonry Wall Behavior Under Cyclic Loading Using Applied Element Method; *Seisan Kenkyu*, Vol. 58, No. 6, pp.531-534
- Sathiparan, N.(2008), Experimental Study on PP-Band Mesh Seismic Retrofitting for Low Earthquake Resistant Masonry Houses, PhD Dissertation, Institute of Industrial Science, The University of Tokyo, Japan
- Ramesh GURAGAIN, Ganesh JIMEE, Amod Mani DIXIT (2008); Earthquake Awareness and Effective Planning through Participatory Risk Assessment: an Experience from Nepal, *14<sup>th</sup> WCEE*, 12-17 October, 2008, Beijing China
- Kawin WORAKANCHANA, Paola MAYORCA, Ramesh GURAGAIN, Sathiparan NAVARATNARAJ and Kimiro MEGURO (2008); 3-D Applied Element Method for PP-Band Retrofitted Masonry; *Seisan Kenkyu*, Vol. 60 No. 2 pp.128-131
- Joonam Park, Peeranan Towashiraporn, James I. Craig and Barry J. Goodnod. (2009). Seismic fragility analysis of low-rise unreinforced masonry structures, *Engineering Structures* **31**. 125-137.
- M. Rota, A. Pennab and G. Magenes. (2010). A methodology for deriving analytical fragility curves for masonry buildings based on stochastic nonlinear analyses. *Engineering Structures* **32**, 1312-1323.